The Impact of Increased Frequency of Rawinsonde Observations on Forecast Skill Investigated with an Observing System Simulation Experiment

N. C. PRIVÉ AND R. M. ERRICO

Goddard Earth Sciences Technology and Research Center, Morgan State University, Greenbelt, Maryland

K.-S. TAI

Science Systems and Applications, Inc., Greenbelt, Maryland

(Manuscript received 19 July 2013, in final form 16 December 2013)

ABSTRACT

Most rawinsondes are launched once or twice daily, at 0000 and/or 1200 UTC; only a small number of the total rawinsonde observations are taken at 0600 and 1800 UTC (''off hour'' cycle times). In this study, the variations of forecast and analysis quality between cycle times and the potential improvement of skill due to supplemental rawinsonde measurements at 0600 and 1800 UTC are tested in the framework of an observing system simulation experiment (OSSE). The National Aeronautics and Space Administration Global Modeling and Assimilation Office (NASA GMAO) Goddard Earth Observing System Model, version 5 (GEOS-5), is used with the GMAO OSSE setup for an experiment emulating the months of July and August with the 2011 observational network. The OSSE is run with and without supplemental rawinsonde observations at 0600 and 1800 UTC, and the differences in analysis error and forecast skill are quantified. The addition of supplemental rawinsonde observations results in significant improvement of analysis quality in the Northern Hemisphere for both the 0000/1200 and 0600/1800 UTC cycle times, with greater improvement for the off-hour times. Reduction of root-mean-square errors on the order of 1%–3% for wind and temperature is found at the 24- and 48-h forecast times. There is a slight improvement in Northern Hemisphere anomaly correlations at the 120-h forecast time.

1. Introduction

Studies have shown that rawinsonde observations have a large impact on forecast skill, particularly in the Northern Hemisphere and tropics (e.g., Zapotocny et al. 2008; Gelaro and Zhu 2009). In most locations, rawinsondes are regularly released once or twice a day at 0000 and/or 1200 UTC, but the operational global forecasts at the National Centers for Environmental Prediction (NCEP) are run 4 times daily at 0000, 0600, 1200, and 1800 UTC. Anecdotally, the 0600 and 1800 UTC forecasts are sometimes considered to have degraded medium-range forecast skill compared to the 0000 and 1200 UTC forecasts, presumably due to the lack of rawinsonde observations and diurnal variation in number of aircraft observations at these analysis times.

During high-impact weather events, supplemental rawinsonde launches at 0600 and 1800 UTC are sometimes performed over portions of the continental United States in an effort to improve forecast skill. Recent examples occurred for Hurricane Irene (2011), when supplemental rawinsondes were launched over the eastern United States, and Hurricane Sandy (2012), when supplemental rawinsondes were launched over the continental United States. Because of the rarity of large-scale supplemental rawinsonde launches, it is difficult to quantify the impact of the extra rawinsonde observations on forecast skill.

This paper will address the analysis quality and forecast skill of off-hour 0600 and 1800 UTC forecast cycles as well as the impact of supplemental rawinsonde observations using an observing system simulation experiment (OSSE). The OSSE framework allows the analysis and forecast quality to be quantified exactly, and synthetic supplemental rawinsonde observations can be added to the analysis cycle at will.

Corresponding author address: Nikki C. Privé, NASA/GSFC, Code 610.1, Greenbelt, MD 20771.
E-mail: nikki.prive@nasa.gov

DOI: 10.1175/MWR-D-13-00237.1

© 2014 American Meteorological Society

The National Aeronautics and Space Administration Global Modeling and Assimilation Office (NASA GMAO) OSSE setup will be described in section 2. The relative quality of the forecast skill at different cycle times will be addressed in section 3 The impact of supplemental rawinsondes will be investigated in section 4. Section 5 will discuss the results, and section 6 will present brief conclusions.

2. OSSE setup

An OSSE has been developed at NASA GMAO that is described in detail by Errico et al. (2013) and Privé et al. (2013); a brief synopsis of the setup will be given here. OSSEs are pure simulation studies in which the real world is replaced by a long free-model run, called the nature run. For the GMAO OSSE, this is a 13-month run of the European Centre for Medium-Range Weather Forecasts (ECMWF) operational model version c31r1, performed at T511 resolution with 91 vertical levels. The nature run starts on 1 May 2005 and ends on 31 May 2006, with 3-hourly output. The sea surface temperature and sea ice fields are prescribed according to the 2005–06 values; all other fields are generated by the ECMWF model. The nature run has been evaluated in comparison to observed climatology, and the synoptic behavior was found to be acceptable for use in an OSSE (Reale et al. 2007; McCarty et al. 2012).

Synthetic observations are created to replicate the observational network used in contemporary operational data assimilation systems (DAS). Conventional observations are generated by interpolating the nature run fields to the locations and times of real observations using archived observational datasets for rawinsondes, aircraft, satellite winds, and other data types. Radiance observations are created using the Community Radiative Transfer Model (CRTM; Han et al. 2006), interpolating the nature run fields for clouds, temperatures, and atmospheric composition for the Advanced Microwave Sounding Unit-A (AMSU-A), the Infrared Atmospheric Sounding Interferometer (IASI), the Atmospheric Infrared Sounder (AIRS), the High Resolution Infrared Radiation Sounder-3 (HIRS-3) and -4 (HIRS-4), the Microwave Humidity Sounder (MHS), the global positioning system radio occultation (GPS-RO), and the Microwave Sounding Unit (MSU) observations to mimic the summer 2011 observational network. Synthetic errors are applied to the generated observations; these errors have been calibrated to yield analysis increment statistics that are similar to real world values using the methods described in Errico et al. (2013) for the 2005 dataset. The synthetic observations have been updated and improved compared to the dataset described in Errico et al. (2013) to emulate a more current version of the global observational network, and verified against DAS performance using real observations from 2011. In the updated observations, advection of rawinsondes during ascent is included in the generation of synthetic rawinsonde data.

In these OSSE experiments, the synthetic observations are fed to the Goddard Earth Observing System, version 5.10.0 (GEOS-5), numerical weather prediction model using the gridpoint statistical interpolation DAS (GSI; Kleist et al. 2009; Rienecker et al. 2008). The GEOS-5 model forecasts are run for 120 h starting at 0000, 0600, 1200, and 1800 UTC daily, using the cubed-sphere grid with 180 grid points along each edge of the cube (roughly equivalent to 0.5° resolution at the equator), with 72 hybrid vertical coordinate η levels. Throughout this manuscript, calculations performed on η levels will be referred to by the corresponding pressure that would occur at that level if the surface pressure were 1000 hPa. The forecast skill of the GMAO OSSE has been found to be slightly higher than forecasts using real data (Privé et al. 2013) with similar results for the updated OSSE version; however, the relative observation impact of different data types is reproduced well in the OSSE.

This study focuses on three regions of interest for calculations of analysis and forecast quality. The first region, NHEX, spans the Northern Hemisphere extratropics from 20° to 60°N, a region that includes the majority of available rawinsonde observations. The second region is that of continental North America (NAM) from 20°–60°N to 140°–60°W, a densely observed area. The third region is the Atlantic Ocean basin (ATL) from 20°–60°N to 60°–10°W, which is not well observed by rawinsondes or other conventional observations but is located downstream from the NAM region.

3. Current state of analysis and forecast skill

For the control case, the OSSE is cycled using the baseline dataset of synthetic observations from 15 June to 5 September 2011. The analyses and forecasts are examined from 1 July to 31 August 2011, discarding the last two weeks of June as spinup. The control case is used to investigate any differences in the quality of the "on hour" (0000 and 1200 UTC) versus "off hour" (0600 and 1800 UTC) analyses and forecasts.

The analysis error can be calculated explicitly within the OSSE setup, since the "truth" is known in the form of the nature run. The root-mean-square error (RMSE) between the analysis state and nature run is calculated at each η level for the Northern Hemisphere extratropics. The two-month mean analysis RMSE is calculated for

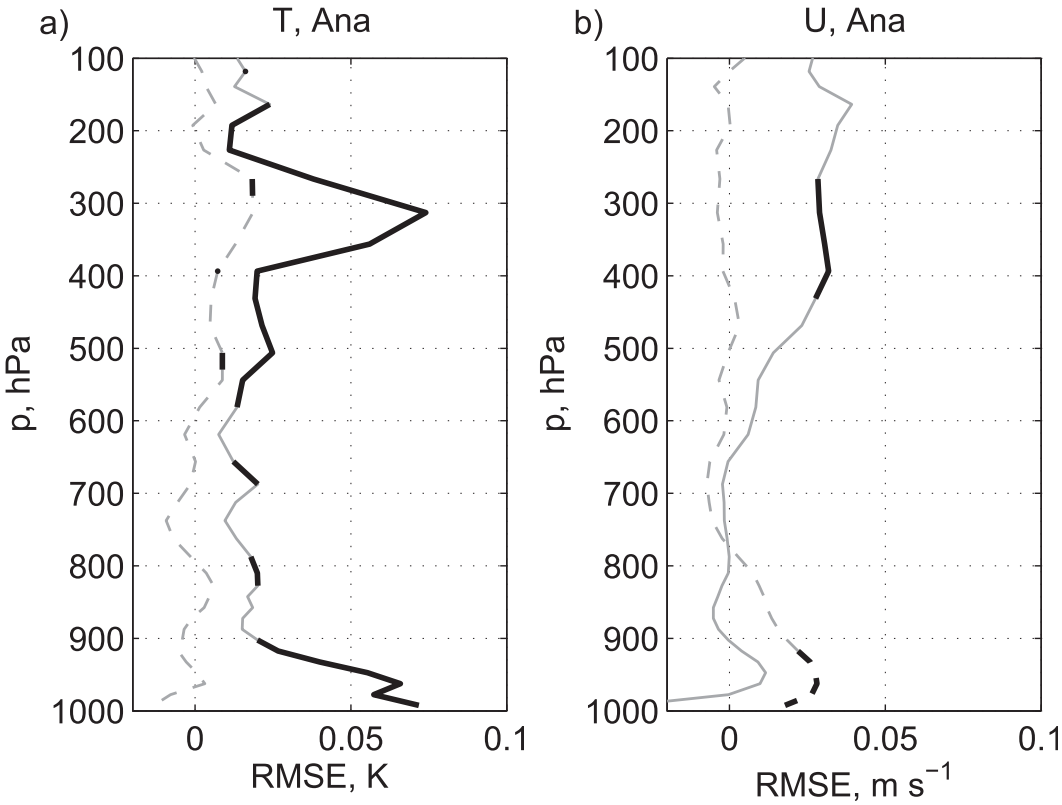

FIG. 1. Difference in time mean analysis RMSE between on-hour (0000 and 1200 UTC) and off-hour (0600 and 1800 UTC) cycle times for the NHEX region: Control case (solid lines) and XRAOB case (dashed lines). (a) Temperature (K) and (b) zonal wind (m s^{-1}). Dark lines indicate a statistically significant difference in the on-hour and off-hour time mean RMSE at greater than 95% confidence level; thin gray lines indicate that significance is below the 95% level. Positive values indicate larger RMSE for the off-hour cycle times compared to the on-hour cycle times.

the on-hour and off-hour cycle times as shown in Fig. 1. In the NHEX region, off hours are found to have statistically significantly larger analysis RMSE for temperature from 600 to 150 hPa than on hours, with significantly greater wind RMSE in the off-hour cycles from 450 to 250 hPa, as shown by the solid dark lines in Fig. 1.

The temporal evolution of the analysis RMSE is also investigated. If the reduction in the quantity of rawinsonde observations at off hours negatively affects the analysis quality, it would be expected that the analysis error would jump up and down, with higher values at 0600 and 1800 UTC and lower values at 0000 and 1200 UTC. An illustration of this behavior is seen in the top panel of Fig. 2, where the time series of both the analysis and background RMSE for temperature on the 312-hPa η surface has a sawtooth appearance. While the analysis RMSE has higher values at off hours, the background RMSE has higher values at on hours. The 6-h lag between the peaks in the analysis and background error is due to the dependence of the background error upon the analysis error of the previous cycle. The time series of zonal wind RMSE has a somewhat smoother appearance (Fig. 2, bottom panel). The jumpiness of the analysis and background has been observed in a previous OSSE study by Errico et al. (2007).

A measure of the "jumpiness" is the autocorrelation R, which is the correlation of a signal with itself at a different point in time:

$$R(\tau) = \frac{E[(X_t - \mu)(X_{t+\tau} - \mu)]}{\sigma^2}, \qquad (1)$$

where τ is the time lag, t is the time, E is the expectation operator, μ is the mean of the signal X, and σ^2 is the variance of X. The autocorrelation is calculated for a 6-h time difference for the analysis at each cycle time; low values of autocorrelation would indicate that the signal is jumpy. The autocorrelation for temperature and zonal wind in the control case are shown as black lines in Fig. 3 for the three different regions of interest.

In general, autocorrelations are relatively high for wind and humidity (not shown) at all cycle times, although low autocorrelations of wind are observed in the lower troposphere. For temperature, low autocorrelations

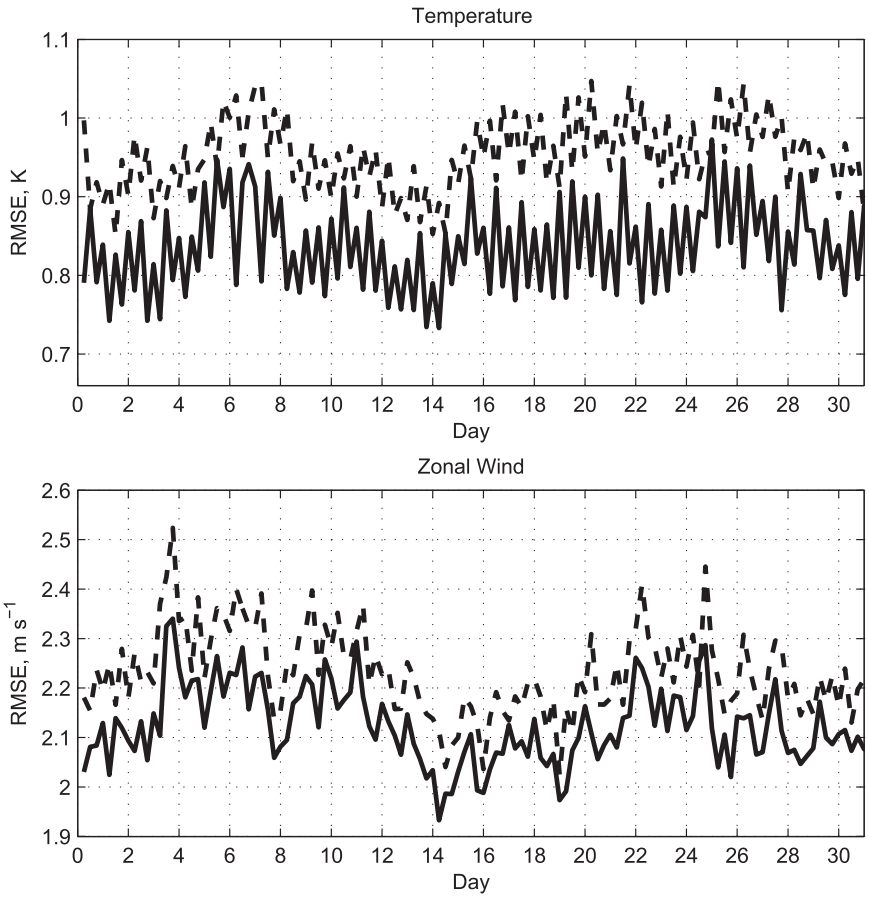

FIG. 2. Time series of area-averaged RMSE from 20° to 60°N on the model surface near 312 hPa over the month of July. Control case (top) temperature (K) and (bottom) zonal wind (m s^{-1}). Analysis error (black line) and background error (dashed line).

are seen from 200 to 400 hPa, particularly in NHEX where the autocorrelation is near zero at the level of the jet stream. In the NAM and ATL regions, the autocorrelation shows a small decrease both near 300 hPa and near 750–800 hPa, but autocorrelations are higher in general than for the NHEX region. There are very few rawinsonde observations in the ATL basin, so jumpiness due to the availability of rawinsonde observations is minimal. Over the NAM region, the observational coverage is very dense so that during off hours, other data types partially compensate for the lack of rawinsondes.

A moist adjoint of the GEOS-5 model has been developed to help estimate the impact of individual observation types on the quality of the 24-h forecast measured using a moist total energy norm, as described by Holdaway et al. (2014). The moist total energy norm is calculated from the surface to 100 hPa as in Ehrendorfer et al. (1999), with parameter ϵ chosen so that the contribution of temperature and specific humidity terms are of similar magnitude. Figure 4 compares the adjoint estimated observation impacts in the NHEX region from 3 to 13 July for the 0000 (black bars) versus 1800 UTC (dark gray bars) cycle times of the control case. As expected, the impact of rawinsondes (Q_RAOB, T_RAOB, and W_RAOB for specific humidity, temperature, and horizontal wind, respectively) are much larger at the 0000 UTC cycle time compared to the 1800 UTC cycle time. At the 1800 UTC cycle time, AMSU-A, AIRS, aircraft temperature, and satellite wind observations have increased observation impact compared to the 0000 UTC cycle time, although these increases are not statistically significant. These increased impacts occur as the observations compensate for the lack of rawinsondes at 1800 UTC, so there is more opportunity for other observing types to do "work." However, the sum of all observing impacts is approximately 25% greater at the 0000 UTC cycle time compared to the 1800 UTC cycle time, implying that the other observing systems are not able to completely compensate for the lack of rawinsondes.

The forecast skill of on- and off-hour initial forecast times is also compared as with the analysis error. All

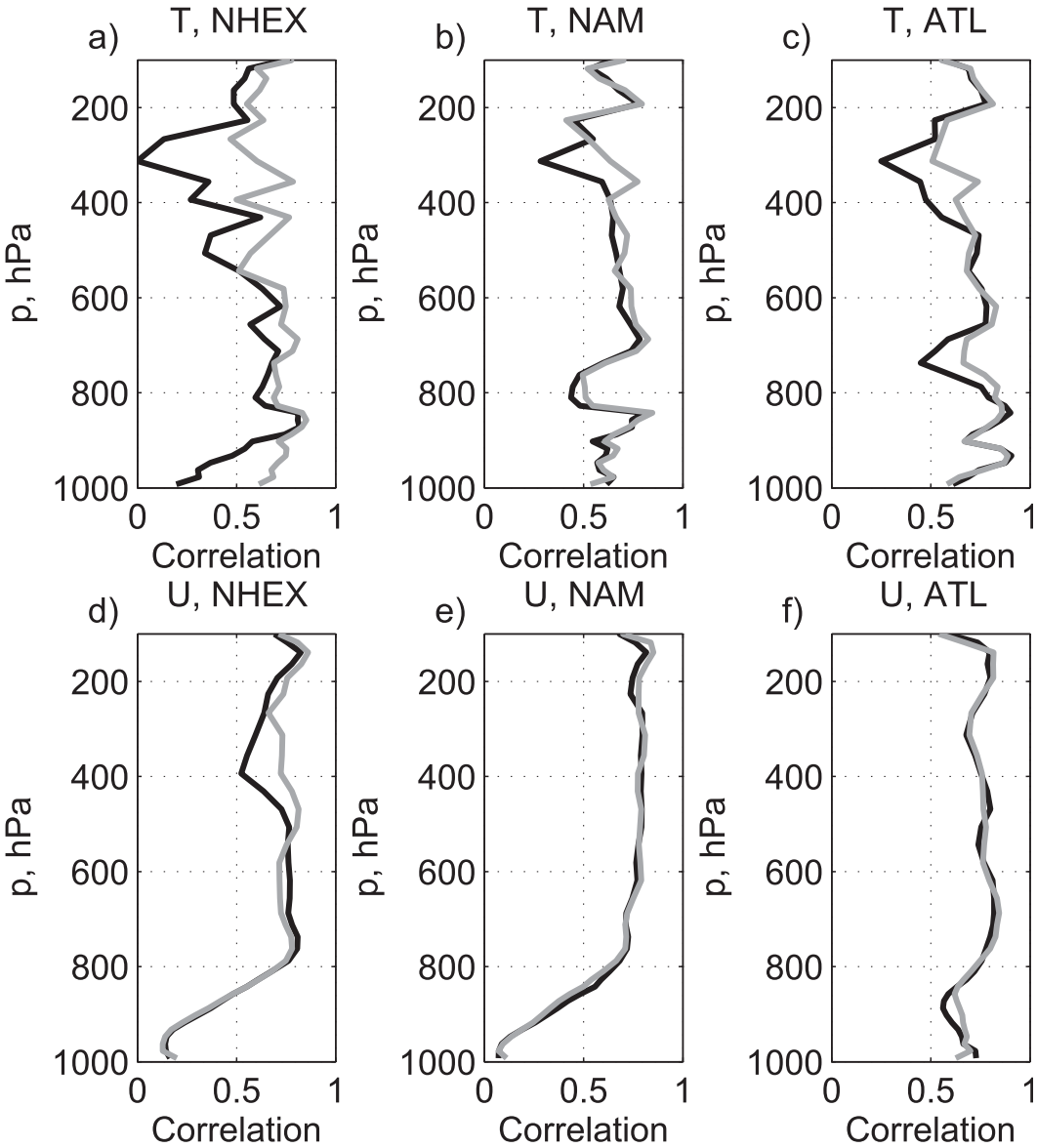

FIG. 3. Autocorrelation of analysis RMSE between the 0000 and 0600 UTC cycle times. Control case (black line) and XRAOB case (gray line). (a),(d) NHEX; (b),(e) NAM; (c),(f) ATL. (top) Temperature and (bottom) zonal wind.

forecast fields are verified against the nature run, rather than using self-analysis verification. The results (not shown) show that forecasts starting at on-hour times have lower RMSE forecast error over the NHEX region at both 24- and 48-h forecast times, but the difference in RMSE is statistically significant only below 900 hPa.

4. Impact of supplemental rawinsondes

Synthetic rawinsonde observations are generated for 0600 and 1800 UTC using a simple algorithm: if a rawinsonde observation was taken during the previous cycle at a particular location, a new observation is generated six hours later at that same location. At locations where rawinsondes are launched only once daily, this results in two launches per day, while at locations where rawinsondes are launched twice daily, four launches will occur. Any rawinsonde observations that normally occur only at 0600 or 1800 UTC and not at the previous cycle time were omitted. These new observations are added to the baseline suite of observations, and the OSSE is again cycled from 15 June to 5 September 2011; this experiment will be referred to as XRAOB. Figure 5 shows the locations of rawinsondes in the control and XRAOB cases for the 0600 UTC 10 July 2011 analysis cycle as an example of the difference in the two cases.

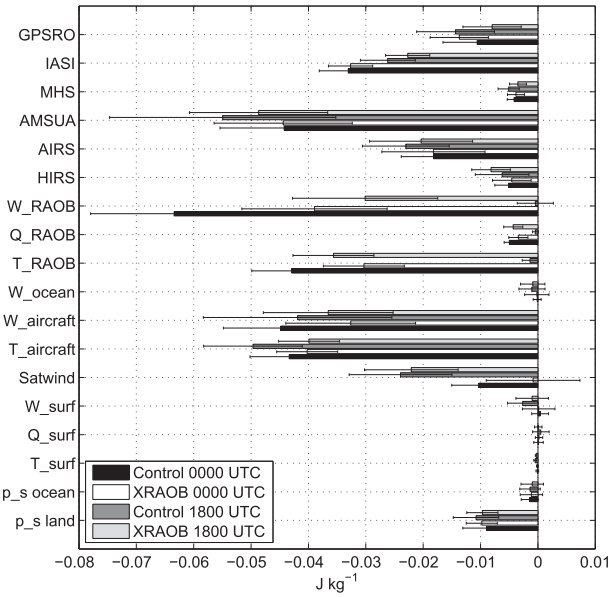

FIG. 4. Adjoint-derived estimate of observation impacts on 24-h forecast of moist energy norm, negative values indicate an improvement of the forecast due to the ingestion of observational data. Barbs indicate 95% confidence intervals. 0000 UTC control case (black bars), 0000 UTC XRAOB case (white bars), 1800 UTC control case (dark gray bars), and 1800 UTC XRAOB case (light gray bars).

Figure 1 shows the difference between on-hour and off-hour two-month mean analysis RMSE for the XRAOB case (dashed lines) in comparison to the control case (solid lines). The difference in analysis RMSE between cycle times is significantly decreased in the XRAOB case compared to the control case. The remaining difference in analysis RMSE between cycle times may be due to the availability of aircraft observations or diurnal variation in atmospheric conditions.

As in the control case, the autocorrelation is calculated for the XRAOB experiment to determine if the supplemental rawinsondes decrease the jumpiness of the analysis error sequence. The gray lines in Fig. 3 illustrate the autocorrelation for the XRAOB case. There is a large increase in the autocorrelation for temperature in the upper troposphere in the NHEX region in comparison to the control case (black lines), implying that the low autocorrelation in the control was due to the lack of rawinsonde observations on the off hours. Smaller increases in upper-tropospheric temperature autocorrelations are seen in the NAM and ATL regions. There is also a significant increase in autocorrelation of temperature near the surface in the NHEX region and near 750 hPa in the ATL region. For zonal wind, the only notable difference in autocorrelation is from 500 to 300 hPa in NHEX, where there is a modest increase in the XRAOB case.

Time series of the analysis RMSE on the 312-hPa η level for temperature and zonal wind are shown in Fig. 6 to compare the control (black lines) and XRAOB (gray lines) cases. The temperature RMSE sequence is smoother with the addition of supplemental rawinsondes, in contrast to the control case, with slightly lower analysis RMSE in the XRAOB case. The zonal wind RMSE is similar in character for both the XRAOB and control cases, with lower overall RMSE and fewer spikes of high error in the XRAOB case.

In addition to reducing the jumpiness of the analysis error, the supplemental rawinsondes change the overall quality of the analysis at all cycle times. Figure 7 shows the difference in monthly mean analysis RMSE between the control and XRAOB cases for the combined off hours (solid lines) and the combined on hours (dashed lines), where positive values indicate a reduction in error in the XRAOB case.

The XRAOB case shows a reduction in analysis temperature RMSE for both on and off hours in all three regions of interest. Greater reduction in analysis temperature RMSE is found for the off-hour cycle times, particularly near the jet stream (near 10% reduction) and in the lower troposphere (2%–5%) in the NHEX and NAM regions. The zonal wind field also shows a reduction in analysis RMSE, with the largest reductions in the NHEX region (up to 3%). The NAM and ATL regions show reduction of zonal wind RMSE of 1%–2%, with statistically significant reductions in the middle and upper troposphere. In the lower troposphere, the on-hour cycles have greater reduction in RMSE than the off hours for zonal wind over land. Over the ATL basin, there is less discrepancy between on- and off-hour reduction in RMSE for both temperature and zonal wind.

The comparison of forecast RMSE between the control and XRAOB cases for wind and temperature in the three regions is calculated for the 24- and 48-h forecasts in Figs. 8 and 9, respectively. For temperature, reduction of RMSE in the XRAOB case is found to be statistically significant at 24 h principally below 500 hPa, with greater reduction in RMSE (2%–4% of total RMSE) at off-hour cycle times compared to on-hour times (1%–2%). At 48 h, the NHEX region shows statistically significant reduction in temperature RMSE below 600 hPa for the off-hour cycle times (1% reduction), but little reduction in RMSE for on-hour times. The NAM region at 48 h does not show statistically significant improvement in temperature RMSE, and the ATL regions shows significant improvement of approximately 2% only for off-hour temperature RMSE between 200 and 400 hPa.

The NHEX region shows statistically significant reduction of RMSE in the XRAOB case for zonal wind at

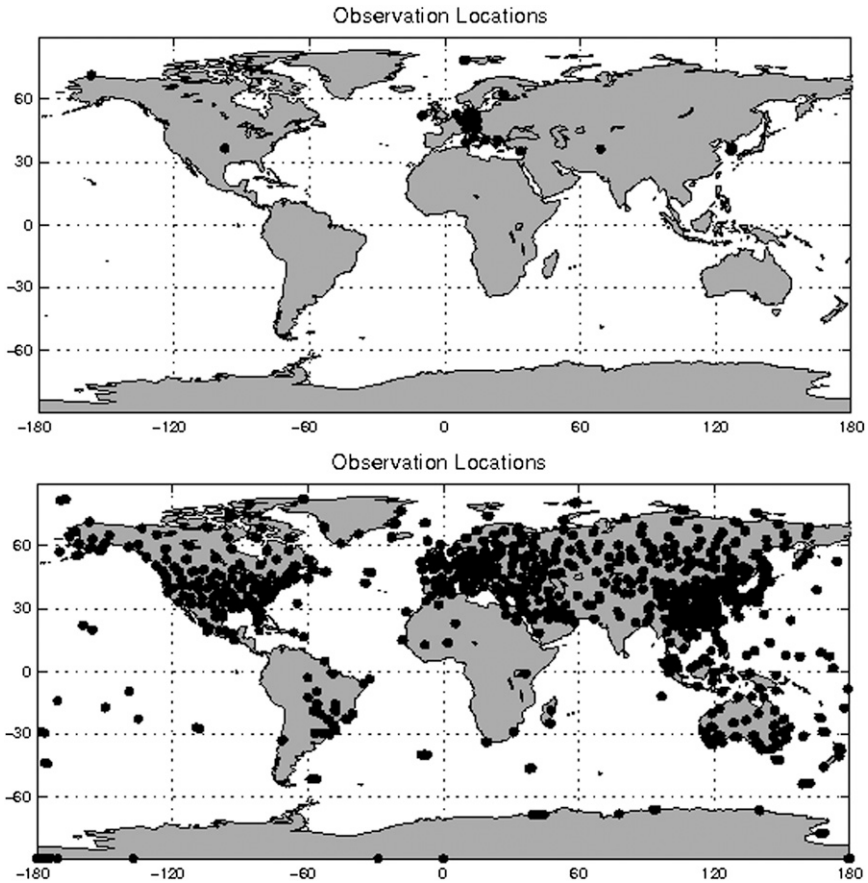

FIG. 5. Location of rawinsonde observations (solid circles) at 0600 UTC 10 Jul 2011. (top) Control case and (bottom) XRAOB case.

both 24 and 48 h in the mid- and upper troposphere for both on- and off-hour cycle times, with a considerably larger reduction (up to 3%) at off-hour times. The NAM region shows statistically significant improvement in forecast RMSE (2%) for zonal wind only for off-hour cycle times in the upper troposphere, while the ATL region shows improvement in zonal wind RMSE for both on and off hours only at the 24-h forecast between 800 and 500 hPa.

Weaker statistical significance of RMSE improvements in the NAM and ATL regions compared to NHEX can be attributed in part to the larger spatial area of NHEX resulting in a less noisy temporal dataset of RMSE, while the small NAM and ATL regions are quite noisy. Spatial maps of analysis and forecast error (not shown) indicate that supplemental rawinsondes have a large impact over eastern Asia and the west Pacific, both areas with limited conventional observations. Some radiance observations (such as channels 1–3 from AMSU-A) are excluded from the DAS over land regions, increasing the importance of rawinsondes over the Asian continent.

The 120-h anomaly correlations of 500-hPa geopotential for the Northern Hemisphere extratropics for the control and XRAOB cases are given in Table 1. A Wilcoxon signed-rank paired test is used to determine the statistical significance of the difference in day-5 anomaly correlation scores between the two cases for the months of July and August. The p values from the Wilcoxon test give the probability that the two sample sets are drawn from distributions with the same median, with values of $p < 0.05$ indicating statistically significant differences in the median at the 95% confidence level. All cycle times show an improvement in skill scores, but only the 0600 and 1200 UTC cycle times have improvements that are significant at greater than 95% confidence.

The adjoint-derived estimate of observation impacts in the Northern Hemisphere extratropics for the 0000 UTC XRAOB case is indicated by the white bars in Fig. 4, while the 1800 UTC XRAOB observation impacts are shown with light gray bars. At 1800 UTC, the rawinsonde impacts are much larger in the XRAOB case compared to the control, as expected. While the

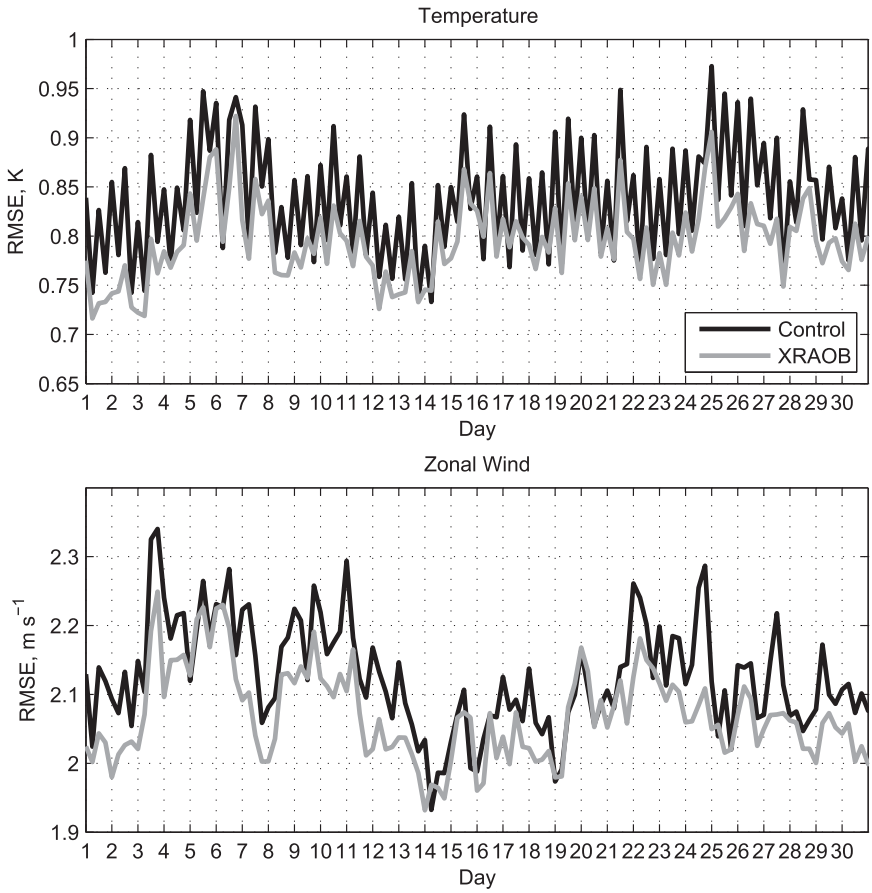

FIG. 6. Time series of area averaged RMSE from 20° to 60°N on the model surface near 312 hPa over the month of July. (top) Temperature (K) and (bottom) zonal wind (m s^{-1}). Control analysis error (black line) and XRAOB analysis error (gray line).

1800 UTC XRAOB rawinsonde impacts are fairly similar in magnitude to the 0000 UTC XRAOB impacts, the rawinsonde impacts for both 0000 and 1800 UTC in the XRAOB case are smaller than for the 0000 UTC control case, particularly for wind impacts. Reduced background error in the XRAOB case due to supplemental rawinsondes yields less ''work'' to be done by the DAS, especially in the vicinity of rawinsonde observations. Thus, the observation impact of rawinsondes at 0000 UTC is decreased in the XRAOB case compared to the control.

Most conventional observation types other than rawinsondes also show decreased impact in the XRAOB case compared with the control, although the magnitudes of the decrease are not statistically significant. The sum of all impacts is approximately 20% smaller for the XRAOB 0000 UTC cycle compared to the control 0000 UTC cycle. However, this sum of impacts is 10% greater in the XRAOB case compared to the control at 1800 UTC, further indicating that the rawinsondes add new information that cannot be compensated for by other instruments in the current observing network. Indeed, if other observing types were able to completely compensate for the lack of rawinsondes at off hours, there would be no improvement to the analysis or forecasts when supplemental rawinsondes are added.

5. Discussion

In the control case, the difference in analysis quality between the on- and off-hour cycle times is small, on the order of 1% difference in zonal wind RMSE and 2%–3% difference in temperature RMSE. At the 0000 and 1200 UTC cycle times, the widespread availability of rawinsonde data can act to reduce large errors that may be present in the subsequent background field, while at 0600 and 1800 UTC, a high-quality background field derived from the previous cycle helps to mitigate the lack of rawinsonde data. Examination of the RMSE of the background fields of wind and temperature verifies

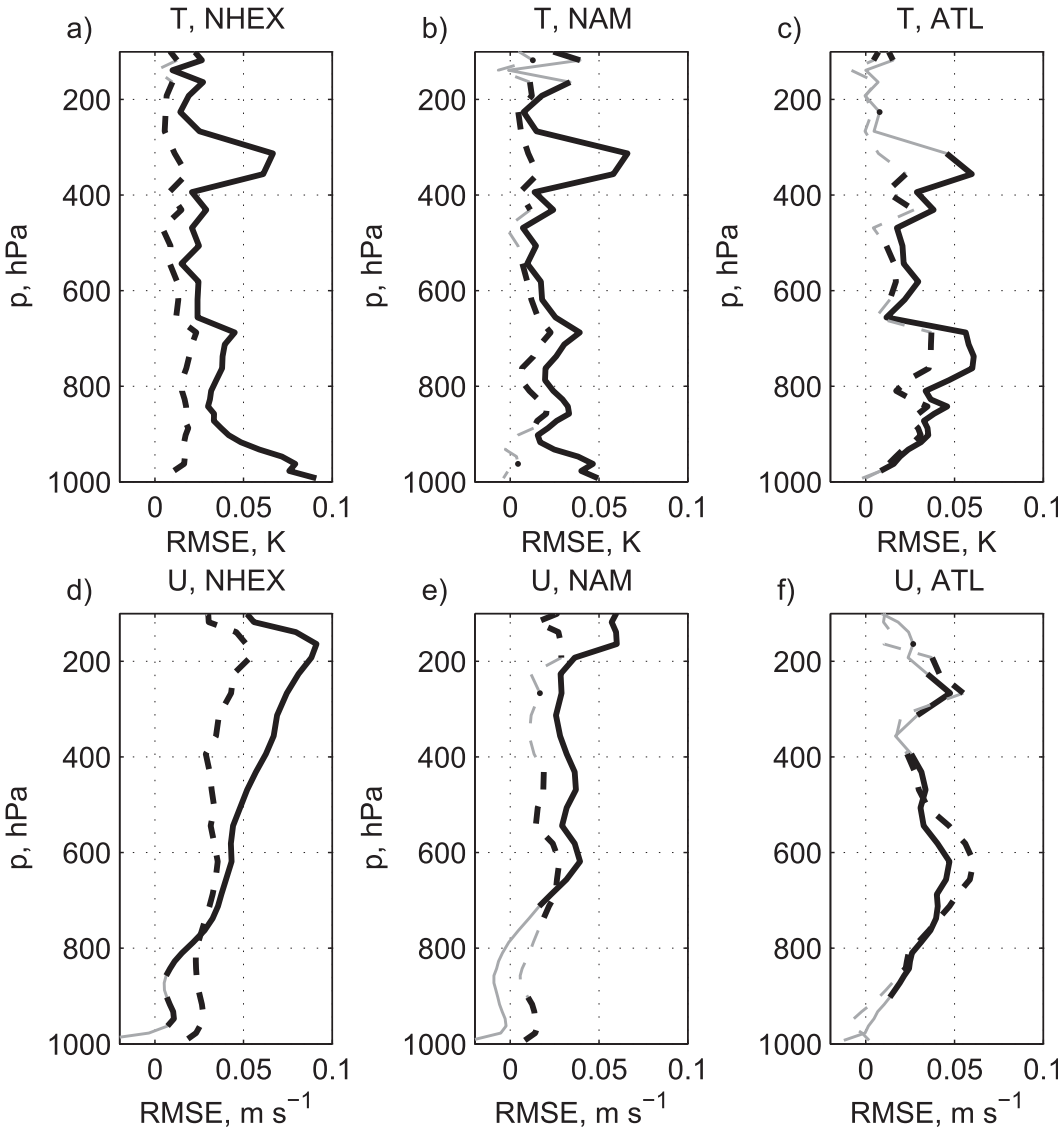

FIG. 7. Difference in root-mean-square analysis error between the control and XRAOB cases for (top) temperature (K) and (bottom) zonal wind (m s^{-1}) for the three regions. Dashed lines indicate combined differences for the 0000 and 1200 UTC cycle times and solid lines indicate combined differences for the 0600 and 1800 UTC cycle times. Black sections of lines indicate statistically significant differences between control and XRAOB at the 95% confidence level and the gray segments indicate statistical significance of less than 95%. (a),(d) NHEX; (b),(e) NAM; (c),(f) ATL.

that the lower background field error occurs for the off-hour cycle times compared to the on-hour cycle times.

One exception is for temperature in the upper troposphere, where there is up to a 10% difference in RMSE between on- and off-hour times. This region may also be influenced by the diurnal pattern of availability of aircraft observations. The large improvement in the upper-troposphere temperature RMSEs when supplemental rawinsondes are added is not retained into the 24- or 48-h forecast times, while improvements in other regions are retained. This rapid ''forgetting'' of the improved analysis state into the early forecast is indicative of model error processes.

Although the improvements to RMSE of wind and temperature due to supplemental rawinsondes were found to be relatively small by the 48-h forecast period, statistically significant improvement to hemispheric anomaly correlation was found for the 0600 and 1200 UTC cycle times. This indicates that the information added by rawinsondes can be retained into the extended forecast period and affect the evolution of the large-scale synoptic patterns measured by the anomaly correlation metric.

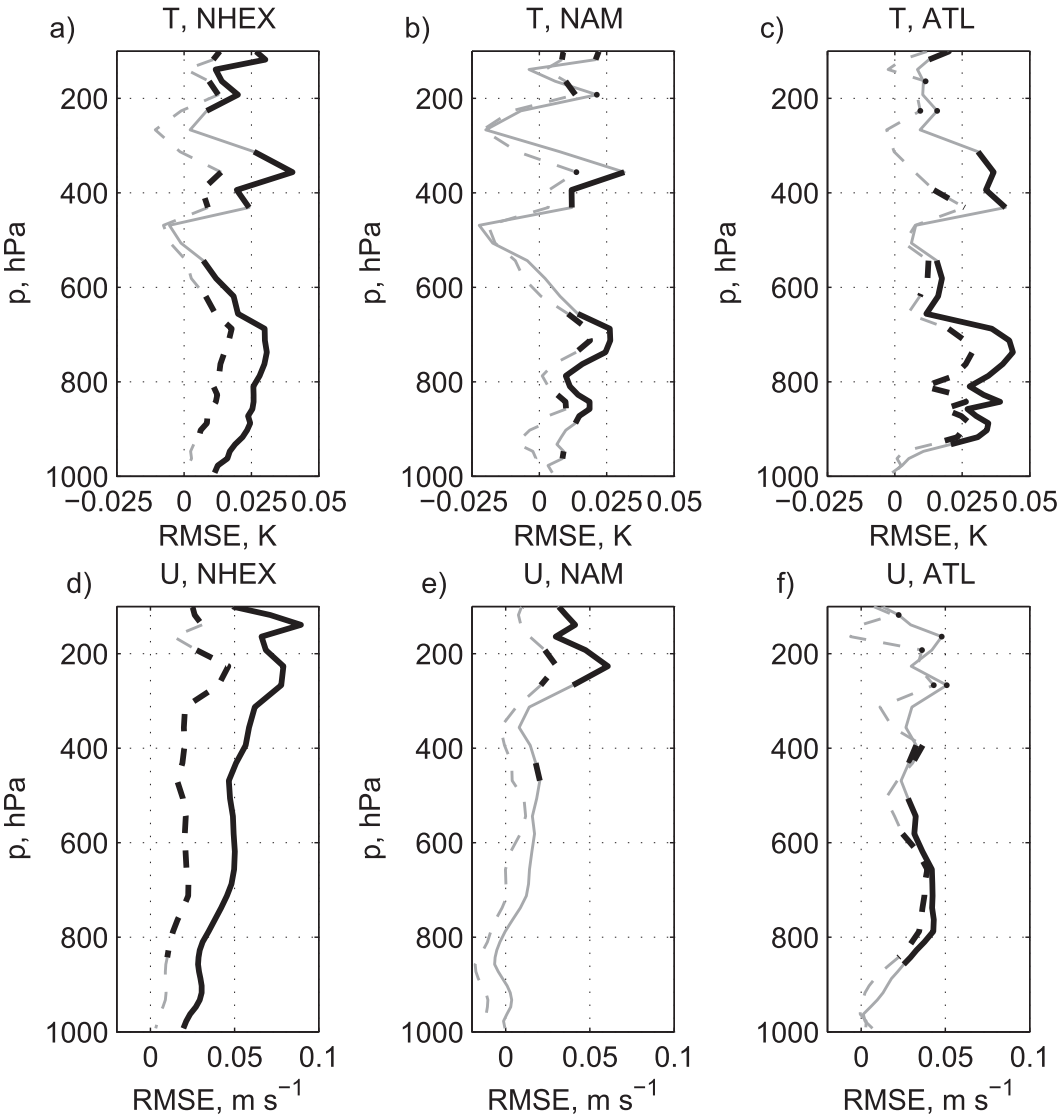

FIG. 8. As in Fig. 7, but for the 24-h forecast error.

Because of the high skill of current operational numerical weather prediction systems, it is difficult to effect a large improvement on anomaly correlation metrics by introduction of new observations.

Supplemental rawinsondes improve not only the off-hour forecast skill and analysis quality, but also the on-hour forecast skill and analysis. By improving the analysis quality of off-hour times, the background quality of on-hour cycle times is also improved (although to a lesser degree), resulting in improved on-hour cycle time analyses. While the NHEX and NAM regions show greater improvement in analysis and forecast RMSE for the off hours compared to the on hours, the ATL region had nearly equal improvement in RMSE at both sets of cycle times. Because there are few rawinsonde stations within the ATL region, improvements to the analysis and forecast states are advected into the ATL from upstream regions, principally from the NAM region because of midlatitude westerlies.

One of the motivations for wide-scale launches of supplemental rawinsondes is to improve forecasts of potential high-impact tropical cyclones in the Atlantic basin. While it is possible to perform a series of case studies of tropical cyclone forecasts using the ECMWF nature run to determine the impact of supplemental rawinsondes on tropical cyclone track forecast skill, these studies must be approached with care. Ideally, an NWP forecast ensemble should be used on both the control and experimental observing network cases to improve the robustness of the experimental results. All of the available tropical cyclones in the region of interest from the nature run should be explored; the worst control

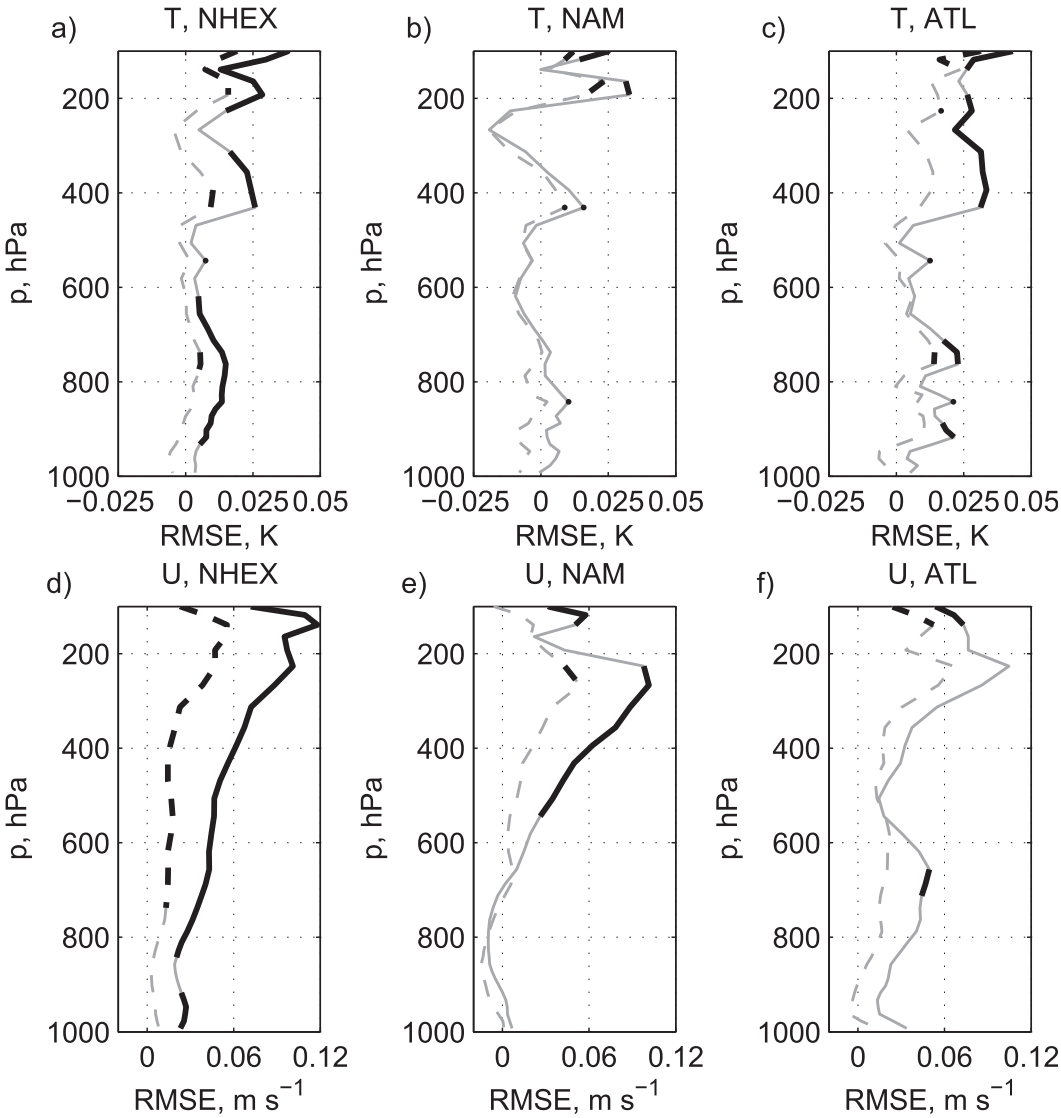

FIG. 9. As in Fig. 7, but for the 48-h forecast error.

forecasts should not be cherry picked for the experiment. The issue of vortex relocation should also be treated with care, with suitable errors introduced into the relocation scheme to mimic realistic uncertainties in the central position and strength of tropical cyclones.

As an ensemble model setup is not available for the GEOS-5 forecasts, and there are only two Atlantic tropical cyclones during the test period, case studies were not performed. Instead, the improvement in anomaly correlation and RMSE are considered as a proxy for improvements in tropical cyclone track forecasts. The improvements to mid- and lower-tropospheric zonal wind RMSE in the ATL region for the 24-h forecast at both on- and off-hour times would be expected to reduce errors in the initial steering forecasts of tropical cyclones.

6. Conclusions

Analysis error is influenced by multiple factors, including the quality and availability of observations, growth or decay of error from the previous analysis, the model error incurred during forward integration from

TABLE 1. Mean 120-h anomaly correlations for Northern Hemisphere extratropical 500-hPa geopotential and Wilcoxon signed-rank test probability p that the control and XRAOB populations have the same median; daily forecasts from 1 Jul to 31 Aug.

	Control	XRAOB	p
0000 UTC	0.863	0.868	0.13
0600 UTC	0.857	0.872	0.00
1200 UTC	0.864	0.872	0.01
1800 UTC	0.863	0.871	0.06

the previous analysis to the current background state, and the ways in which the observations are used by the DAS. Rawinsonde observations are heavily weighted in data assimilation systems and these observations provide vertical sounding observations that are often not available from other data types. As demonstrated by the adjoint estimates of observation impact, other data types are only able to partially compensate for a lack of rawinsonde data.

Supplemental rawinsonde releases at 0600 and 1800 UTC result in a small but statistically significant improvement in analysis quality and forecast skill on both hemispheric and regional scales. While off-hour cycle times feel the greatest improvement from supplemental rawinsondes, on-hour cycle times benefit from the improved background state from the previous off-hour cycle forecast. The additional information provided by supplemental rawinsondes is communicated to oceanic regions during forward integration of the NWP, and at least some information is retained into the medium-range forecast period.

There are several limitations of this study. Only the boreal summer season has been explored here; impacts in the Northern Hemisphere midlatitudes may differ during the winter season when baroclinic activity is more vigorous. Much more extensive testing would be needed to examine the impact of supplemental rawinsondes on specific phenomena such as tropical cyclones, convection, and synoptic-scale systems.

Acknowledgments. The ECMWF nature run was provided by Erik Andersson through arrangements made by Michiko Masutani. Support for this project was encouraged by Michele Rienecker and provided by GMAO core funding. Helpful comments from three anonymous reviewers led to significant improvements in this manuscript.

REFERENCES

Ehrendorfer, M., R. Errico, and K. Raeder, 1999: Singular-vector perturbation growth in a primitive equation model with moist physics. *J. Atmos. Sci.,* **56,** 1627–1648, doi:10.1175/1520-0469(1999)056<1627:SVPGIA>2.0.CO;2.

Errico, R. M., R. Yang, M. Masutani, and J. Woollen, 2007: The estimation of analysis error characteristics using an observation systems simulation experiment. *Meteor. Z.,* **16,** 695–708, doi:10.1127/0941-2948/2007/0242.

——, ——, N. Privé, K.-S. Tai, R. Todling, M. Sienkiewicz, and J. Guo, 2013: Validation of version one of the Observing System Simulation Experiments at the Global Modeling and Assimilation Office. *Quart. J. Roy. Meteor. Soc.,* **139,** 1162–1178, doi:10.1002/qj.2027.

Gelaro, R., and Y. Zhu, 2009: Examination of observation impacts derived from observing system experiments (OSEs) and adjoint models. *Tellus,* **61A,** 179–193, doi:10.1111/j.1600-0870.2008.00388.x.

Han, Y., P. van Delst, Q. Liu, F. Weng, B. Yan, R. Treadon, and J. Derber, 2006: JCSDA Community Radiative Transfer Model (CRTM), version 1. NOAA Tech. Rep. 122, 40 pp.

Holdaway, D., R. Errico, R. Gelaro, and J. G. Kim, 2014: Inclusion of linearized moist physics in NASA's Goddard Earth Observing System data assimilation tools. *Mon. Wea. Rev.,* **142,** 414–433, doi:10.1175/MWR-D-13-00193.1.

Kleist, D., D. Parrish, J. Derber, R. Treadon, W.-S. Wu, and S. Lord, 2009: Introduction of the GSI into the NCEP global data assimilation system. *Wea. Forecasting,* **24,** 1691–1705, doi:10.1175/2009WAF2222201.1.

McCarty, W., R. Errico, and R. Gelaro, 2012: Cloud coverage in the joint OSSE nature run. *Mon. Wea. Rev.,* **140,** 1863–1871, doi:10.1175/MWR-D-11-00131.1.

Privé, N., R. Errico, and K.-S. Tai, 2013: Validation of forecast skill of the Global Modeling and Assimilation Office observing system simulation experiment. *Quart. J. Roy. Meteor. Soc.,* **139,** 1354–1363, doi:10.1002/qj.2029.

Reale, O., J. Terry, M. Masutani, E. Andersson, L. Riishojgaard, and J. Jusem, 2007: Preliminary evaluation of the European Centre for Medium-range Weather Forecasts (ECMWF) nature run over the tropical Atlantic and African monsoon region. *Geophys. Res. Lett.,* **34,** L22810, doi:10.1029/2007GL031640.

Rienecker, M., and Coauthors, 2008: The GEOS-5 data assimilation system—Documentation of versions 5.0.1, 5.1.0 and 5.2.0. Tech. Rep. NASA/TM-2008-104606, Vol. 27, NASA, 118 pp. [Available online at http://gmao.gsfc.nasa.gov/pubs/docs/Rienecker369.pdf.]

Zapotocny, T., J. Jung, J. L. Marshall, and R. Treadon, 2008: A two-season impact study of four satellite data types and rawinsonde data in the NCEP global data assimilation system. *Wea. Forecasting,* **23,** 80–100, doi:10.1175/2007WAF2007010.1.